An HTS flux pump operated by directly driving superconductor into flux flow region in the *E-J* curve

Jianzhao Geng and T. A. Coombs

Department of Engineering, University of Cambridge, Cambridge, CB3 0FA, United Kingdom
E-mail: jg717@cam.ac.uk

Abstract

High T_C Superconducting (HTS) flux pumps are capable of compensating the persistent current decay in HTS magnets without electrical contact. In this paper, following the work of an LTS self-switching flux pump, we propose a new HTS flux pump by directly driving high T_C superconductor into flux flow region in the *E-J* curve. The flux pump consists of a transformer which has a superconducting secondary winding shorted by an YBCO coated conductor bridge. A high alternating current with much higher positive peak value than the negative peak value is induced in the secondary winding. The current always drives the bridge superconductor into flux flow region only at around its positive peak value, thus resulting in flux pumping. The proposed flux pump is much simpler than existing HTS flux pumps.

1 Introduction

High-T_c Superconducting (HTS) Coated Conductors (CCs) are ideal candidates for use in high field magnet. They have high critical field as well as good mechanical properties [1]. The widely application of CCs magnets, however, is impeded by the fact that they cannot at present work in persistent mode. This is because on the one hand a lossless joint is hard to achieve [2], and on the other hand loss is induced when an HTS magnet is in the presence of an external oscillating field [3]. One way to solve the problem is to use an external power supply to operate the magnet, but thick current leads have to be used for transporting high current, which induces considerable heat loss [4]. The use of current leads is even more challenging if the magnet were to be moving, such as in the case of a rotor winding. An alternative solution is to use a flux pump. Flux pumps [5]-[17] are devices which can inject flux into a superconducting circuit without electrical contact. HTS flux pumps are capable of charging the magnet and compensating any current decay, enabling the quasi-persistent current operation of CCs magnets [18].

Low T_c superconducting (LTS) flux pumps have been studied for decades, most of which can be found in the review papers of [5], [6]. Basically, these flux pumps rely on intermittently driving at least part of the superconductor normal. HTS flux pumps have only recently been developed. These flux pumps include, rectifier flux pumps [7]-[10], linear travelling flux pumps [11]-[13], rotating permanent magnets based flux pumps [14]-[17]. Rectifier flux pumps rely on the effective control of HTS switch (switches), either by heat [7], biased DC field [8], and AC field of low frequency [9], [10] or of radio frequency [19]. In our previous work [20], we made a general analysis on HTS flux pumps, especially travelling wave based flux pumps. We have theoretically proven that it is not necessary to drive high T_c superconductors normal to achieve flux pumping. It is the variable resistivity of high T_c superconductors that results in flux pumping. Resistivity

appears in superconductor when there is flux motion, for example flux flow. Flux flow occurs when a superconductor is subjected to an ac field, transporting an alternating current, or transporting a direct current above its critical current. In Ref. [9], we have described a flux pump which is based on ac field triggered flux flow. In Ref. [21], [22], the authors proposed a self-switching LTS flux pump, which depends on driving superconductor normal by driving current above the critical value. Following their work, in this paper, we will show that for an HTS flux pump, it can also work by driving high T_c superconductor in CC into flux flow region in the *E-J* curve [23]. The performance of the flux pump under different operating conditions will also be presented.

2 Basic principle

As shown in Fig. 1(a), a varying magnetic field is applied to an HTS loop which includes a resistive joint. An alternating current $i(t)$ circulating the loop is induced by the field. A superconducting load L which we want to magnetize is connected to branch *ab* which has a much lower critical current than the rest of the HTS loop. If there is a continuous net flux flow across branch *ab*, there is an associated voltage $v(t)$ across branch *ab* which has a DC value. Flux accumulates in the load L and it can be charged [20]. In the following we will explain how the net flux flow across branch *ab* is achieved. If we properly coordinate the resistance and inductance of the HTS loop, as well as the changing rate of the applied field, we can achieve an asymmetrical $i(t)$ which has zero DC value. The *V-I* curve of branch *ab* and one example waveform of the periodical circulating current $i(t)$ is plotted together in Fig. 1(b). During each cycle of $i(t)$, at region A and only region A, the critical current of the superconductor I_c has been exceeded and a voltage developed across the load. The remainder of the waveform is arbitrary save that $abs(i(t))<I_c$ and the integration of $i(t)$ over each period is zero. Therefore, during each cycle, there is a net flux flowing across branch *ab*, and the dc voltage across branch *ab* is non-zero. The superconducting load inductor connected to branch *ab* is hence gradually charged.

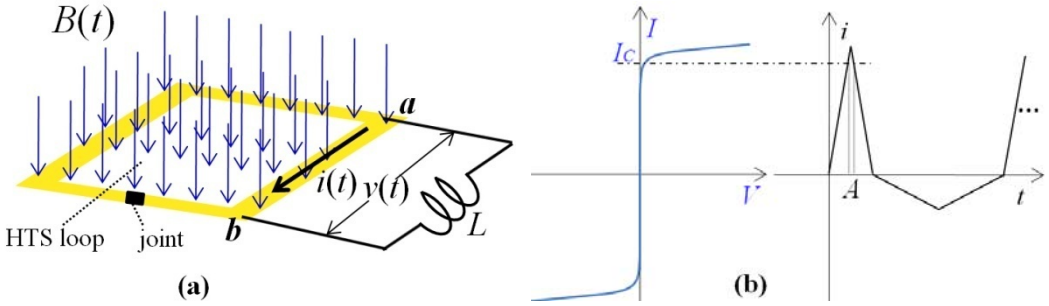

Fig. 1. Basic principle of the proposed HTS flux pump. (a) A varying magnetic field is applied to an HTS loop which consists of a resistive joint. A superconducting load L is connected to branch *ab* which has a smaller critical current value than the rest of the HTS loop. (b) the V-I curve of branch *ab* (left), and one example waveform of the circulating current $i(t)$ (right). During each cycle of $i(t)$, at region A and only region A the critical current of branch *ab* has been exceeded and a voltage developed across the load. For the remainder of the waveform, $abs(i(t)) < I_c$.

3 Experimental system

An experimental system was built up, as shown in Fig. 2(a). A 100:1 transformer was used to induce an alternating current with high magnitude in its secondary winding. The secondary

winding was made of parallel YBCO tapes with a total critical current of 360A. Two ends of the secondary winding were soldered together via another piece of YBCO tape which we refer to as "the bridge". The bridge length was 10cm and it had a critical current of 180A. The bridge was also used to short an YBCO double pancake load coil. The inductance of the coil was 0.388mH. The critical current of the coil was 81A. Other specifications of the coil can be found in [24]. All above critical current values were measured at the temperature of 77k with the criterion of E_0=10^{-4}V/m. The whole superconducting system was immersed in Liquid Nitrogen (LN_2).

The primary winding of the transformer was powered by a KEPCO-BOP 2020 power amplifier. The KEPCO was controlled by an NI-USB 6002 data acquisition card which can output programmable analogue signal from LabVIEW. The KEPCO worked in current mode, which means that output current is proportional to the input signal. In this way we were able to generate a desirable primary current. The primary current i_1 was measured via a 0.5 ohm resistor, the secondary current i_2 was monitored by an open loop Hall Effect current sensor, load current i_L was measured by a pre-calibrated hall sensor fixed at the center of the load coil. All analogue signals were sampled by the NI-USB 6002 card, with a sampling rate of 400Hz. The load current data were filtered by averaging every 5 continuous samples.

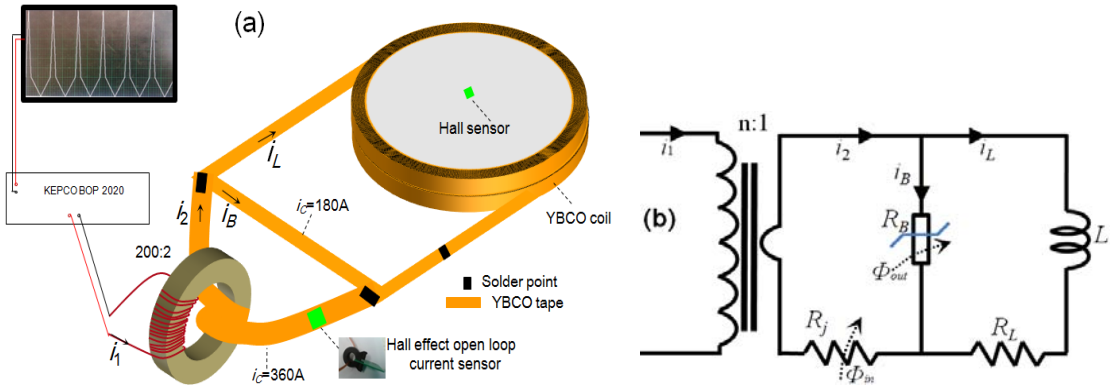

Fig. 2 Schematic drawing of the proposed flux pump and its equivalent circuit. (a) Schematic experimental system. A transformer generates an asymmetrical current in its secondary winding which is shorted by the bridge. The bridge has a lower current capacity than the winding. When the secondary current i_2 exceeds the critical current of the bridge, flux will flow to the load via the bridge. (b) Circuit analogue of the system, where R_j denotes joint resistance, R_B denotes flux flow resistance of the bridge superconductor. The flux flow direction has also been drawn in the circuit.

The equivalent circuit of the system is shown in Fig. 2(b). R_j represents joint resistance in the secondary winding, R_B denotes flux flow resistance of the bridge superconductor, R_L is an equivalent resistance in the load loop which includes joint resistance and other losses, and L is the load inductance. The bridge inductance is too small to be considered. It should be noted that the joint resistance R_j is essential to damp down any direct current component in the secondary winding, otherwise the transformer iron core might be saturated. In the experiment, the total joint resistance was estimated to be R_j=10$\mu\Omega$. From a circuit point of view, the proposed flux pump is similar to the LTS flux pump in Ref. [21]. However, they are distinct from each other in terms of physics and control strategy. The origin of R_B in the manuscript is due to flux flow [23] of high-T_c superconductor, while in Ref. [21] it depends on driving low-T_c superconductor normal.

4 Experiments and Result

4.1 Primary current setting and charging details

In the experiment, we have used an alternating triangular signal as the primary current i_1. During the period when i_1 is positive, i_1 ramps up to a peak value I_{1pp} at a constant rate, and then ramps down with the same rate to zero; during the period when i_1 is negative, i_1 ramps down to a negative peak value of $-I_{1np}$, and then ramps up with the same rate to zero again. The length of positive period over the length of negative period is inversely proportional to I_{1pp}/I_{1np}, thus making the dc component in i_1 equals to zero, i.e.:

$$\int_0^T i_1(t)dt = 0 \qquad (1)$$

Where T is the period of i_1.

In the following experiment, the controllable parameters include the current positive peak value I_{1pp}, the negative peak $-I_{1np}$, and the current frequency f. Fig. 3 shows two waveforms with the same peak values but at different frequencies.

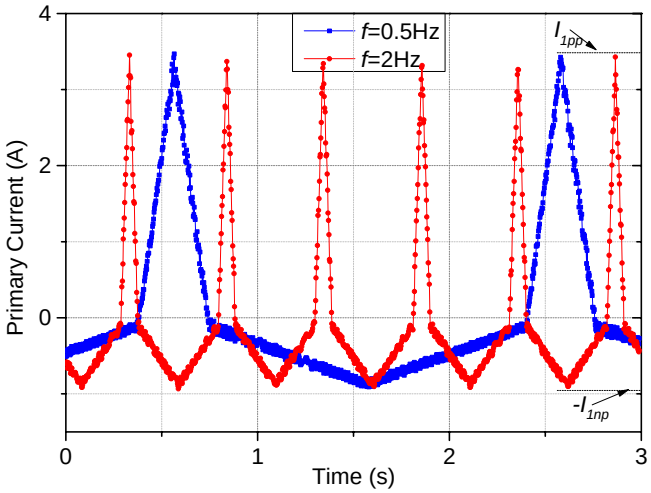

Fig. 3 Waveform of primary current of the transformer i_1, with frequency f=0.5Hz and f=2Hz. I_{1pp} denotes the positive peak value of i_1, and $-I_{1np}$ denotes the negative peak value of i_1.

Fig. 4 shows the detailed waveform of bridge current i_B and the load current i_L. The positive peak current of i_B is about 250A, and the negative peak value of i_B is around -100A. The critical current of the bridge superconductor i_C is 180A, which is in between the positive peak value and the negative magnitude (absolute value). As can be seen from Fig. 4, at each period when the bridge current exceeds i_C, the load current increases by about 3A; during the rest of i_B cycle, the load current nearly remains stable. The average voltage across the bridge can be expressed as:

$$V = \frac{1}{T_{ff}} \Delta i_L \times L \qquad (2)$$

Where T_{ff} represents the duration when the bridge superconductor is in flux flow region in each current cycle, and it is about 0.1s in Fig. 4. Δi_L denotes the current increase in each cycle, and it is estimated to be 3A. L is the inductance of the load which is 0.388mH.

According to the above numbers, the voltage V is estimated to be 11.64mV. The electric field is

then calculated to be 1.16mV/cm. If all the current had migrated to the cooper layer, the electric field would be much larger than 1.16mV/cm. Therefore the superconductor is far from normal.

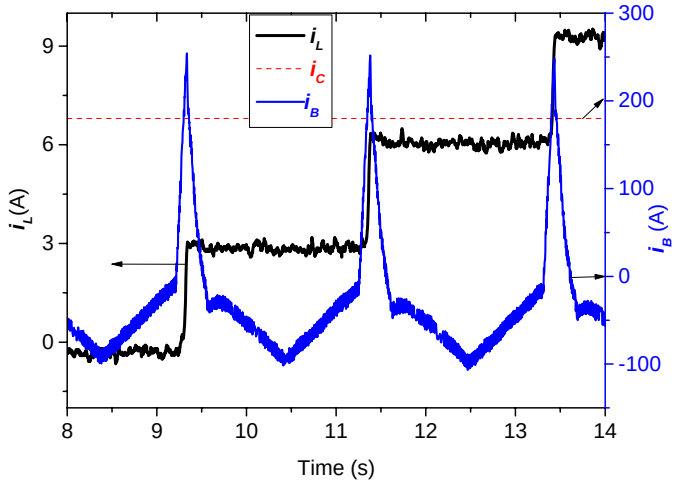

Fig. 4. Detailed Waveform of bridge current i_B, load current i_L, and critical current of the bridge.

4.2 Load current under different primary current magnitudes

For an ideal transformer, its secondary current i_2 is always proportional to the primary current i_1. However, for a real transformer, if the load impedance is high, the output voltage may reach its limit so that the secondary current cannot follow the primary current. In this section, we will study the influence of primary current magnitude on the load current, since the bridge resistance originally depends on the primary current.

If the positive peak of primary current I_{1pp} is relatively too low to make the bridge voltage reach the limit, then the secondary current is proportional to the primary current with a ratio of 100:1. The charging curve is shown in Fig. 5. At the beginning of the charging process, the secondary current i_2 equals to bridge current i_B because load current i_L is zero. With the increase of i_L, i_B is gradually biased to the opposite direction. In this case the bridge dc voltage also drops with the increase of load current. Therefore, the load current presents a curve which is like the charging curve of a first order circuit. When I_{1pp} is too low to drive the bridge to flux flow region, the load current tends to saturate at a value which is lower than the critical current of the load coil. Fig. 5 shows the case where the load current i_L saturated at 40A when i_B reduced to about 180A (the critical current of the bridge).

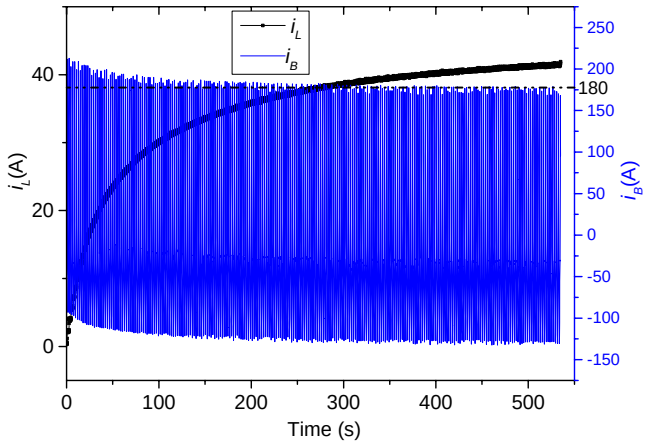

Fig. 5 Waveform of bridge current i_B and load current i_L during the whole charging process. The primary current is low, so that the bridge current i_B reduces with the increase of load current. The load current cannot reach the critical current of the coil. It stabilizes at a level where the positive peak value of the bridge current approximately equals to the critical current of the bridge.

In contrast, when the primary current level is too high, the bridge voltage will reach its limit. This means that the bridge dc voltage in each cycle nearly remains constant. In this case, the positive peak value of the bridge current remains constant during the whole charging process as well. The charging process is shown in Fig. 6. During each cycle, the load current increases by the same amount, so the load current's rate of change is nearly constant until it reaches the critical current of the load coil, which is 81A in the experiment.

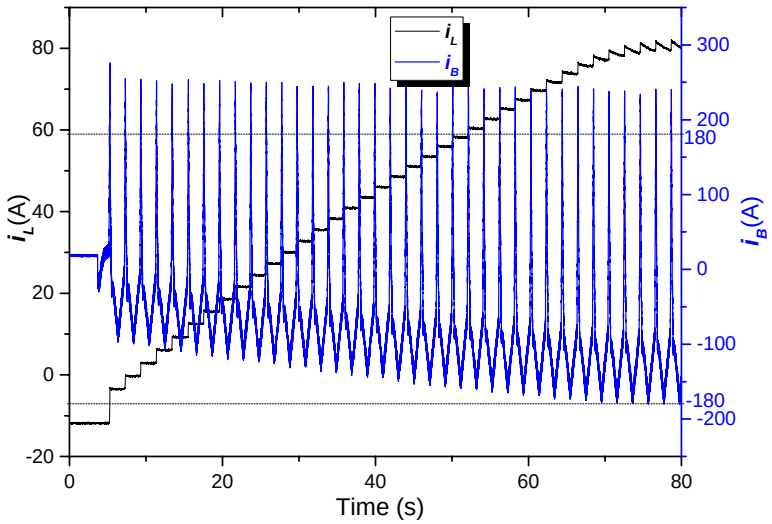

Fig. 6 Waveform of bridge current i_B and load current i_L during the whole charging process. The primary current is high, so that the bridge voltage is always limited by the capacity of the transformer during the whole charging process. The load current curve is nearly linear before reaching the critical current of the load coil.

It should be noted that no matter whether the primary current is high or low, the negative magnitude (the absolute value) of the bridge current will increase with the increase of the load current. In the experiment, the load coil critical current is 81A, and the critical current of the

bridge is 180A. To make sure that the negative magnitude of the bridge current will not exceed 180A, the negative magnitude of the secondary current should be less than 99A. Fig. 6 shows the actual case where the load current reaches the critical value, and at the same time the negative magnitude of the bridge current reaches the bridge critical current.

Fig. 7 shows the load current curves under different primary current magnitudes. In all experiment, the negative magnitude of the primary current I_{1np} is set to be 1A.

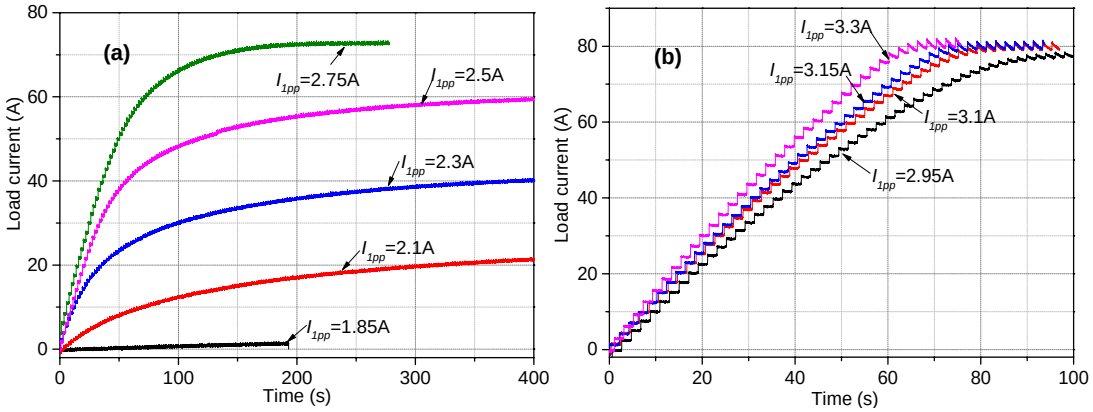

Fig. 7 Load current curves under different positive peak values of primary current I_{1pp}. The negative magnitude in all measurements is set as I_{1np}=1A. The frequency of the primary current is 0.5Hz.

4.3 Load current under different primary current frequencies

In this part of experiment, our aim is to test the frequency dependence of charging performance. During each measurement, the shape of the primary current was fixed. The frequency of primary current varies from 0.5 Hz to 16Hz. The waveform of primary current is shown in Fig. 3, where I_{1np}=1A, I_{1pp}=3.3A. Higher frequency was not tested due to the limitation of the KEPCO.

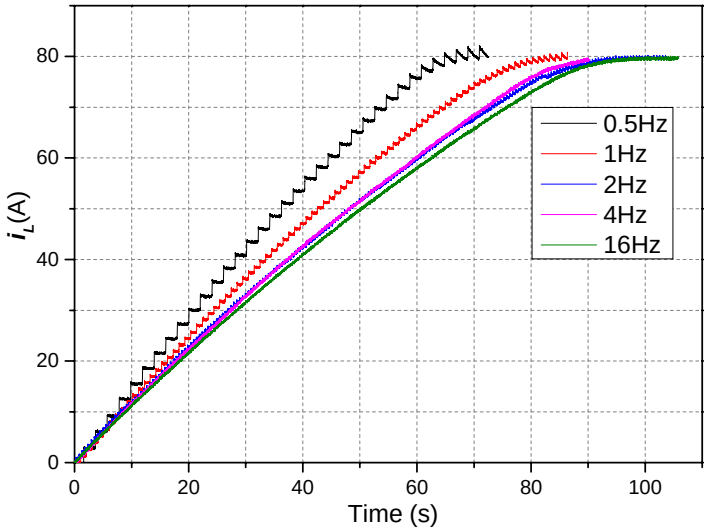

Fig. 8 Load current curves under different frequencies of primary current.

It can be seen from Fig. 8, all load currents saturate at about the critical current of the load coil, but the speed differs a little bit. The fastest charging is under 0.5Hz, followed by the 1Hz case, and the rest curves are nearly overlapped. Theoretically all curves should overlap together, if the *v-i* relationship of the bridge superconductor is independent of current frequency. This is because the waveforms of the primary current are the same except for the frequency, which means the amount of flux flow into the load should be the same during the same time period. However, in practice,

the *v-i* relationship of the bridge superconductor depends on temperature. The flux flow during a certain time can be described as:

$$\phi = \int_0^P v(i,\ T)dt \qquad (3)$$

Where ϕ is the flux flow into the load, $v(i,\ T)$ denotes the instantaneous bridge voltage which depends on the bridge current i and temperature T, and time period P can be multiples of 2s (the period of 0.5Hz signal). It is understandable that lower frequency means a longer continuous time when the superconductor is in flux flow region during each ac cycle, and it is therefore easier for heat to accumulate in the bridge to cause a temperature rise (This is why the bridge superconductor cannot carry a dc as high as the peak value of the ac in the bridge @ 77K). Temperature rise promotes flux flow and shifts the *v-i* curve. Therefore, at lower frequency, the integration in Eq. 3 has a larger value, and the flux pumping is faster.

5 Discussions

All previous HTS flux pumps needs either moving parts [14]-[17] or effective control of switches [7]-[13]. In most of these works magnetic fields have to be applied perpendicular to an HTS tape (tapes), which is difficult to achieve if the field magnets are outside the cooling system. Having field magnets in the cooling system, however, means more loss, especially for the moving ones. In contrast, the proposed flux pump only needs a single transformer to achieve flux pumping. It is not difficult to place the primary winding and the iron core of the transformer outside the cryogenic system. In this way the loss can be significantly reduced. The proposed flux pump is especially suitable for fast pumping up current in large magnets. The main limitation on pumping speed in this flux pump is the capacity of the transformer. In terms of field stability, however, this flux pump may not be very ideal. Because of the sharp V-I curve of the bridge superconductor, it is difficult to achieve an effective control of the bridge voltage. A small noise in the bridge current may induce a large error in the bridge voltage. To solve the problem, it is desirable to combine this flux pump with the dynamic resistance controlled flux pump [9], [10], in which case this flux pump can be used to ramp up the load current and the dynamic resistance controlled flux pump can be used to stabilize the final field.

6 Summary and conclusion

In this paper, we have presented the principle and experimental results for an HTS flux pump. The flux pump consists of a transformer with a superconducting secondary winding which is shorted by a piece of YBCO coated conductor referred as “the bridge”. The transformer generates a high secondary current with its positive peak value much larger than the negative peak value. During each cycle, around the positive peak of the secondary current, the bridge superconductor is driven into the flux flow region, during the rest of the cycle the bridge remains superconducting. Flux is then accumulated in the load.

We tested the performance of the flux pump under different primary current magnitudes and frequencies. The results show that the performance is more dependent on the primary current magnitude but less on the current frequency. The load current can be easily charged to the critical value. The work makes flux pumping for HTS CC coils much simpler than ever before.

This work can also be considered as a fulfillment of the principle for HTS flux pumps we proposed in Ref. [20], in which we predicted that flux pumping might be achieved by a

homogeneous field applying to a superconducting loop with an asymmetrical geometry.

Acknowledgements

Jianzhao Geng would like to acknowledge Cambridge Trust for offering the Cambridge International Scholarship to support his study in Cambridge.

References

[1] M. Sugano, K. Osamura, W. Prusseit, R. Semerad, T. Kuroda, K. Ito, T. Kiyoshi, IEEE Trans. Appl. Supercond. **15**, 3581 (2005).

[2] Y. Park, M. Lee, H. Ann, Y. H. Choi, and H. Lee, NPG Asia Materials, **6** e98 (2014).

[3] Y. G. Park et al, Phys. Proc. **58**, 268 (2014).

[4] Ballarino A 2013 Current leads, links and buses Proc. of the CAS-CERN Accelerator School: Superconductivity for Accelerators (Erice, Italy) (doi:10.5170/CERN-2014-005.547).

[5] L. J. M. van de Klundert and H. H. J. ten Kate, Cryogenics **21**, 195 (1981).

[6] L. J. M. van de Klundert and H. H. J. ten Kate, Cryogenics **21**, 267 (1981).

[7] M. P. Oomen, M. Leghissa, G. Ries, N. Proelss, H. W. Neumueller, F.Steinmeyer, M. Vester, and F. Davies, IEEE Trans. Appl. Supercond. **15**, 1465 (2005).

[8] S. Ishmael, C. Goodzeit, P. Masson, R. Meinke, and R. Sullivan, IEEE Trans. Appl. Supercond. **13**, 693 (2008).

[9] J. Geng and T. A. Coombs, Appl. Phys. Lett. **107**, 142601 (2015).

[10] J. Geng, K. Matsuda, L. Fu, B. Shen, X. Zhang, and T. A. Coombs, Supercond. Sci. Technol. **29**, 035015 (2016).

[11] Y. D. Chung, I. Mut, T. Hoshino, T. Nakamura, and M. H. Shon, Cryogenics **44**, 839 (2004).

[12] Z. Bai, G. Yan, C. Wu, S. Ding, and C. Chen, Cryogenics **50**(10), 688 (2010).

[13] L. Fu, K. Matsuda, and T. A. Coombs, IEEE Trans. Appl. Supercond. **26**, 0500304 (2016).

[14] C. Hoffmann, D. Pooke, and A. D. Caplin, IEEE Trans. Appl. Supercond. **21**, 1628 (2011).

[15] T. A. Coombs, J. F. Fagnard, and K. Matsuda, IEEE Trans. Appl. Supercond. **24**, 8201005 (2014).

[16] Z. Jiang, K. Hamilton, N. Amemiya, R. A. Badcock, and C. W. Bumby, Appl. Phys. Lett. **105**, 112601 (2014).

[17] C. W. Bumby, Zhenan Jiang, J. G. Storey, A. E. Pantoja, and R. A. Badcock, Appl. Phys. Lett. **108**, 122601 (2016).

[18] C. W. Bumby, et al, Supercond. Sci. Technol. **29**, 024008 (2016).

[19] V. F. Solovyov, and Q. Li, Appl. Phys. Lett. **103,** 032603 (2013).

[20] J. Geng, et al, J. Phys. D: Appl. Phys. **49** 11LT01 (2016).

[21] H. L. Laquer, K. J. Carroll, and E. F. Hammel, Phys Lett. **21**, 397(1966).

[22] K. J. Carroll, Cryogenics **13**(6), 353 (1973).

[23] J. Rhyner, Physica C **212**(3-4), 292 (1993).

[24] J. Geng, et al, IEEE Trans. Appl. Supercond. **26**, 10.1109/TASC.2016.2540166.